Optimization of Protein-Protein Interaction Measurements for Drug Discovery Using AFM Force Spectroscopy

Yongliang Yang, Bixi Zeng, Zhiyong Sun, *Member, IEEE,* Amir Monemian Esfahani, Jing Hou, Nian-Dong Jiao, *Member IEEE,* Lianqing Liu, *Member IEEE,* Liangliang Chen, Marc D. Basson, Lixin Dong, *Member IEEE,* Ruiguo Yang, *Member IEEE,* and Ning Xi, *Fellow, IEEE*

***Abstract*— Increasingly targeted in drug discovery, protein-protein interactions challenge current high throughput screening technologies in the pharmaceutical industry. Developing an effective and efficient method for screening small molecules or compounds is critical to accelerate the discovery of ligands for enzymes, receptors and other pharmaceutical targets. Here, we report developments of methods to increase the signal-to-noise ratio (SNR) for screening protein-protein interactions using atomic force microscopy (AFM) force spectroscopy. We have demonstrated the effectiveness of these developments on detecting the binding process between focal adhesion kinases (FAK) with protein kinase B (Akt1), which is a target for potential cancer drugs. These developments include optimized probe and substrate functionalization processes and redesigned probe-substrate contact regimes. Furthermore, a statistical-based data processing method was developed to enhance the contrast of the experimental data. Collectively, these results demonstrate the potential of the AFM force spectroscopy in automating drug screening with high throughput.**

***Index Terms*—Bionanotechnology, Nanosensors, Force spectroscopy, Atomic force microscopy, Protein-protein interactions.**

I. Introduction

The productivity of drug discovery has been an increasing concern in the past decade. Its limitations challenge the current business model of the pharmaceutical industry, and hinder the development of drugs for orphan diseases and diseases prevalent in undeveloped countries [1-3]. In the early stage of drug discovery, screening is applied to identify the "hits" from a library or from newly designed candidate drugs [4, 5]. The screening efficiency and effectiveness significantly affect the total productivity of drug discovery [6, 7]. To address this problem, many assays have been developed to screen compounds for pharmaceutical purposes. Biophysically, nuclear magnetic resonance (NMR), surface plasmon resonance (SPR), and isothermal titration calorimetry have been widely used [8]. Many biochemical assays, such as enzyme-linked immunosorbent assays (ELISA), fluorescence polarization, and fluorescence resonance energy transfer (FRET) are also common for this purpose [8].

Protein molecules mostly assemble together as a supramolecular complex to fulfill their physiological functions [9]. Playing a central role in physiological and pathological processes [10, 11], protein-protein interactions thus provide a rich source of potential therapeutic targets in drug discovery [12, 13]. Compared with traditional therapeutic targets, such as enzymes and G protein-coupled receptors, the interface of protein-protein interactions is large, often highly hydrophobic or charged. These unique characteristics of protein-protein interactions challenge the widely used high-throughput screening technologies mentioned above [14]. Each of these technologies has its own strengths and weaknesses, but some weaknesses are common to many. Some of the methods require fluorescence labelling, which changes the biophysical characteristics of the target proteins [15]. In addition, these methods have high false positive rates in testing protein-protein interactions [16]. Thus, an urgent and significant need exists for developing an effective and efficient method for screening protein-protein interactions [3, 17].

Since its emergence, nanotechnologies have been impacting screening in drug discovery [18, 19]. Among them, atomic force microscopy (AFM) was one of the earliest to be applied to drug discovery [20-23]. Not only can AFM image protein

Manuscript received May 20th, 2018.

R. Yang acknowledges the funding from the Nebraska Center for Integrated Biomolecular Communication (NIH National Institutes of General Medical Sciences P20 GM113126), from Nebraska Center for Nanomedicine (P30 GM127200), from NSF award 1826135.

Y. Yang, Z. Sun, L. Chen, L. Dong, and N. Xi are with the Department of Electrical and Computer Engineering, Michigan State University, East Lansing, MI, 48823, USA. Currently, Z. Sun and N. Xi are affiliated with Department of Industrial and Manufacturing Systems Engineering, The University of Hong Kong, Hong Kong, China. Y. Yang is currently with the Department of Biomedical Engineering, Michigan State University. (N. Xi: xining@hku.hk)

B. Zeng and M. D. Basson are with Departments of Surgery and Biomedical Sciences, University of North Dakota, Grand Forks, ND, 58202, USA.

J. Hou is with School of Information and Control Engineering, Shenyang Jianzhu University, Shenyang 110168, China.

N. Jiao and L. Liu are with State Key Laboratory of Robotics, Shenyang Institute of Automation, Chinese Academy of Sciences, Shenyang, 110006, China.

A. M. Esfahani and R. Yang (ryang6@unl.edu) are with the Department of Mechanical and Materials Engineering, University of Nebraska Lincoln, NE 68588 USA.

molecules *in situ* to investigate their morphology[24], but it is also capable of measuring protein-protein interactions with pico-Newton (pN) resolution [25-29] to study their nanomechanical and adhesion properties [28-30]. This method was also used to analyse protein unfolding [29] and its structure characteristics [31]. AFM based force spectroscopy, quantifying the binding strength of protein affinity, has been considered as one of the promising candidates for drug screening [7, 32]. Using this method, the fluorescence staining process can be avoided, and the low false positive rate can be achieved. Moreover, it can be equipped with other capabilities to achieve the high throughput needed for screening. A high-throughput drug discovery screening technique based on AFM force spectroscopy requires parallel and automated operations as well as integration with other biosensing technologies. To run the screening in parallel, the AFM system can be upgraded from a single cantilever to a cantilever array. In addition, the protein samples can also be patterned into arrays using state-of-the-art patterning methods [33]. At present, several of these capabilities have been realized [34-36].

The application of AFM force spectroscopy on drug discovery suffers from low signal to noise ratio (SNR) as compared with other methods (Table 1). Since drug screening aims to test whether the compounds promote or inhibit protein-protein interactions, the SNR in screening large number of interactions is more important than accuracy. Though AFM force spectroscopy measures single molecular interactions with high resolution, a sufficient analysis requires hundreds of force curve measurements due to this low SNR.

Table I SNR OF DRUG SCREEN METHODS

Technologies	SNR
AFM force spectroscopy [37] [38]	< 10
bioluminescence resonance energy transfer [39]	10
SWATH-mass spectrometry [40]	> 20
surface plasmon resonance biosensor [41]	30
single molecular plasmonic biosensor [42]	> 100
click chemistry enabled screening [43]	> 10000

Hence in this study, as initial steps toward developing an efficient screening method for inhibitors of protein-protein interactions, the process of AFM force spectroscopy was optimized to improve SNR. The characterization of Akt1 binding to FAK was selected as a prototypical example because of the clinical relevance of this molecular pair. Cancer cells upregulate their adhesiveness in response to physical forces, such as increased extracellular pressure and shear stress [44]. In this pathway, the binding of protein kinase B (Akt1) to focal adhesion kinase (FAK) is a critical step [45]. This biochemical response occurs in a variety of cancer types, including adenocarcinomas [45], squamous cell carcinomas [46], and even sarcomas [47]. Indeed, perturbing the interaction between FAK and Akt1 can substantially improve tumour-free survival in a mouse model [48]. Functionalizing FAK to an AFM probe and immobilizing Akt1 to a substrate, we first sought to improve the chemical functionalization method to minimize non-specific bindings. In addition, the AFM tip-substrate contact regimes were redesigned to ensure a robust interaction between the target molecules, including tip-substrate contact level and time, as well as the tip moving speed. Furthermore, we developed a novel data processing method based on statistical analysis to enhance SNR and the contrast between control and experimental samples. Equipped with an AFM based nanorobotics platform, this development will pave the way for high throughput screening in drug discovery.

II. Materials and Methods

A. Materials and reagents:

APTES ((3-Aminopropyl) triethoxysilane), N,N-Diisopropylethylamine (DIEA), triethylamine (TEA) and chloroform were purchased from Sigma Aldrich (St. Louis, MO). NHS-PEG-MAL was purchased from JenKem Technology (Plano, TX). SATP (N-succinimidyl-S-acetylthiopropionate) and secondary antibody for fluorescence detecting were from Thermo Fisher Scientific (Waltham, MA). Akt1 molecules were purchased from Origene (Rockville, MD). PD-10 columns were purchased from GE Healthcare Life sciences (Pittsburgh, PA). The AFM system used in this research was a Bioscope from the Bruker (Santa Barbara, CA). AFM probes were also purchased from the Bruker.

B. AFM probe functionalization

To measure molecular interactions, the two proteins of interest were coated onto an AFM probe and a flat substrate, respectively. In this study, silicon nitride cantilevers with a spring constant of ~0.06 N/m were used. Before each experiment, the spring constant of the cantilevers was measured using the thermal tuning method [49]. The tip functionalization method was developed by H Schindler *et al*. [10].

First, the AFM probe was cleaned in chloroform for an hour. Cleaned probes were rinsed in fresh chloroform and blown dry by argon gas. Probes were then processed in an oxygen plasma cleaner to enhance the hydroxyl group density on the silicon nitride surface. APTES was subsequently coated onto the plasma treated AFM probes via gas phase deposition in a chamber filled with argon gas (APTES, 45 µl, DIEA, 15 µl). The APTES coated probes were then functionalized with PEG linker protein with its two ends grafted by NHS- and MAL-groups (NHS-PEG-MAL). The PEG linker molecule-coated AFM probes were incubated in SATP-functionalized FAK (target protein) molecules for 2-3 hours. The functionalized probes were rinsed three times with phosphate buffered saline (PBS), and then stored in PBS at 4°C before use. To graft the FAK molecule with SATP, SATP solution was mixed with FAK solution, with the molar concentration of SATP 10 times higher than that of FAK to ensure that all FAK molecules were functionalized. After incubating the SATP-FAK mixture for 15 minutes, the solution was then eluted through a PD-10 column. 500 µl of SATP-FAK solution was dipped into a PD-10 column each time for 9 times. The 7^{th} and 8^{th} eluates were collected for usage.

C. Substrate functionalization

Akt1 molecules were directly deposited onto polystyrene (PS) substrate via hydrophobic interactions [50, 51]. Before each experiment, Akt1 molecules were incubated on the surface of a petri dish for 2 hours, and the dish was rinsed with PBS. Due to the hydrophobicity of polystyrene substrate, the Akt1 molecules were coated onto a local region of the petri dish surface. Regions without coating in the same dish were used as a negative control. In another experimental condition, the Akt1 molecules were deposited via APTES linker molecule. Fresh mica substrates were first functionalized by APTES, by the same procedure described in the AFM probe functionalization section above. The Akt1 molecules then bind to the amino groups of APTES molecules.

D. Immunofluorescence staining

To visualized substrate functionalization, FAK molecules were deposited on to APTES coated mica substrate and polystyrene substrate. After coating, the samples were blocked in 5% BSA solution for 1 hour. Following this, the samples were incubated in secondary fluorescence antibody solution for 1 hour in dark. The secondary antibody was Goat anti-Mouse Secondary Antibody with Alexa Fluor 488 from Invitrogen. The samples were rinsed with PBS for three times, and five minutes each time. After that, the samples were imaged with Nikon fluorescence microscope TE1000 (Nikon Instruments Inc., Melville, NY, the USA). The images were captured by CoolSNAP HQ2 CCD Camera (Photometrics, Tucson, AZ), and processed using ImageJ (NIH, Bethesda, MD)

E. AFM based single molecular measurement

In this research, FAK molecules were fixed onto an AFM tip, while Akt1 was deposited onto a flat substrate. In the force spectroscopy experiment, forces rupturing the FAK-akt1 binding were measured by the deflection of the AFM cantilever. The rupture force of molecular pairs relaxed the AFM cantilever deflection during the retraction process, as represented by the sudden drop in measured force. To reduce the influence of capillary forces, and maintain the native conformation of protein molecules, AFM force spectroscopy experiments were performed in PBS. The moving range of the AFM probe was confined within 200 nm. The force spectroscopy was set to trigger mode with a triggering threshold of 5 nm. This parameter was also optimized ranging from 1 nm to 10 nm. For each experimental condition, a 20 by 20 array of spots was probed with a 500 nm pitch size. The tip moving velocity and contact level of the AFM tip were optimized in this study. The binding force was calculated using a customized script in MATLAB (MathWorks Inc.).

III. Results

A. Optimizing substrate functionalization to reduce non-specific bindings

APTES has been widely used as a linker molecule to functionalize the surface of mica, silicon or silicon nitride substrates [52-54]. In aqueous solutions, however, APTES molecules aggregate [55]. This uneven distribution will be translated to the non-uniform distribution of the protein molecules of interest, Akt1 (Fig. 1 (a)). In addition, APTES

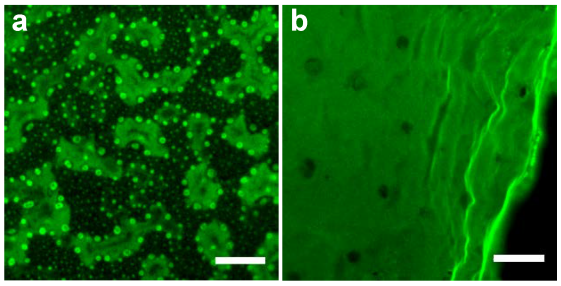

Fig. 1. Directly depositing Akt1 molecules on polystyrene substrate improves the distribution of molecules on the substrate. (a) Fluorescence imaging of Akt1 molecules deposited onto an APTES functionalized mica substrate. (b) Fluorescence image of Akt1 molecules deposited onto a fresh polystyrene substrate. Scale bar: 10 μm.

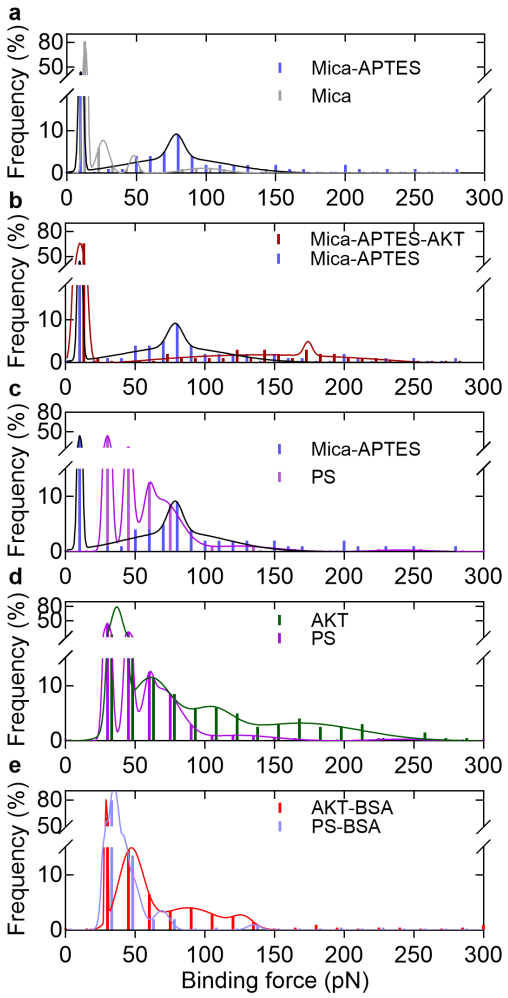

Fig. 2. Optimization of substrate functionalization method to reduce non-specific bindings. The Y axis, frequency, defines the ratio of data points in a specific binding force range and the total data points plotted. (a) Histogram of binding forces between FAK and APTES functionalized mica, and between FAK and fresh mica. (b) Histogram of binding forces between FAK and APTES functionalized mica, and between FAK and Akt1 on APTES functionalized mica. (c) Histograms of binding forces between FAK and PS (polystyrene), and between FAK and APTES functionalized mica. (d, and e) BSA blocking inhibits non-specific binding between FAK and Akt1 molecules. Histogram of binding forces between FAK and Akt1 molecules without (d) and with (e) BSA blocking on PS substrate.

molecules are positively charged under physiological conditions, which increases their electrostatic interactions with the negative charged protein molecules on the AFM probe. Both factors increase the probability of undesired non- specific bindings. On APTES-coated substrates, the measured binding force between FAK molecules and the substrate increased significantly compared with data from substrates without APTES coating (Mica-APTES, Fig. 2 (a)). Depositing Akt1 molecules onto APTES coated mica substrates changed the distribution of binding force (Mica-APTES-AKT, Fig. 2 (b)). The 10 pN peak rose to more than 60% in magnitude, signifying that non-specific binding events were amplified. The Akt1 molecules grafted on top of APTES significantly suppressed the binding probability of FAK to APTES. The peak located at around 80 pN (in Mica-APTES, Fig. 2(b)), representing the binding force between FAK and APTES molecules, disappeared. Meanwhile, the FAK-Akt1 interactions require specific orientations of the two molecules. Thus, the binding probability of FAK-Akt1 is much lower than that of FAK-APTES. This increases the percentage of non-specific bindings, the peak at 10 pN. Further, due to the large binding force of FAK-APTES, the two distributions overlap significantly, making it difficult to distinguish the two interactions (Fig. 2 (b)).

To avoid the undesired bindings caused by APTES, Akt1 molecules were then deposited onto a fresh polystyrene (PS) substrate directly. The hydrophobic interactions of Akt1 with the PS substrate are much stronger than the specific binding between FAK and Akt1. Akt1 molecules that are directly deposited onto fresh PS substrates exhibit significantly improved uniformity compared with Akt1 molecules binding to APTES functionalized PS substrates (Fig. 1 (b)). In addition, non-specific binding forces between the substrate and the FAK molecules increased from 10 pN in mica-APTES substrate to 30 pN in fresh PS substrate. However, the strong interactions between FAK and APTES were avoided (Fig. 2 (c)). Thus, it is easy to distinguish the interactions of FAK-Akt1 and FAK-PS. Binding forces in FAK-PS were mainly restricted in the range smaller than 80 pN (PS, Fig. 2 (d)), while a large portion of FAK-Akt1 binding forces were greater than 80 pN. (AKT, Fig. 2 (d)).

In this drug discovery scenario, the signal here means interaction between FAK and Akt1 via specific interactive binding sites. Besides the strong non-specific binding forces from APTES, the non-specific binding between FAK and Akt1, and FAK and substrate also limited the SNR. Bovine serum albumin (BSA) has been widely used in immunofluorescence staining and western blotting to reduce the non-specific binding. In the context of AFM force spectroscopy, BSA coating to PS substrates increased the percentage of the non-specific binding forces at 30 pN in the experimental group from 45% (PS, Fig. 2 (d)) to 80% (PS-BSA, Fig. 2 (e)). However, BSA blocking also reduced the possibilities of FAK-Akt1 interactions in experimental group, which decreased their binding forces (Fig. 2 (e)). The peak in the histogram is at 75 pN. In both cases, the non-specific binding maintained as ~30 pN. Overall, the SNR was improved dramatically by coating the protein uniformly onto substrate and blocking with BSA.

B. Optimizing AFM tip-substrate interaction

The molecules on AFM tip interact with their counterparts on the substrate when they contact with each other. The characteristics of their contact regime, along with the mechanism of molecular interactions, determines the measured inter molecular forces. To improve the SNR, three parameters of the contact regime were optimized: level and time of AFM tip-substrate contact, and AFM tip moving speed during tip-substrate separation. The values used during experiments are provided in Table II.

TABLE II
PARAMETERS OF CONTACT REGIME

Parameter	Contact level	Contact time	Tip moving speed
Contact level (nm)	1, 3, 5, 10	5	5
Contact time (ms)	No delay	500, 1000	1000
Tip moving speed (nm/s)	100	100	100, 200, 400
Tip moving distance (nm)	200	200	200

Each column is an experimental condition during optimization.

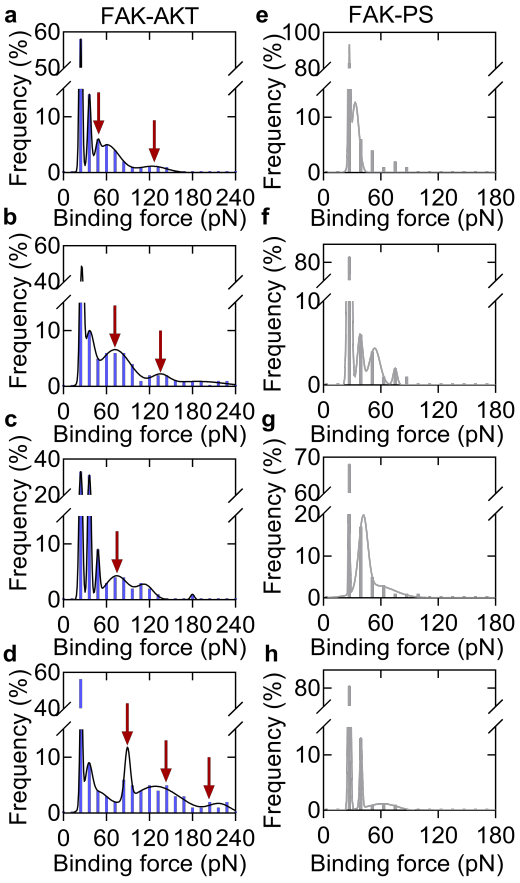

Fig. 3. Optimization of the AFM tip contact level: increasing tip contact level increases the binding forces in FAK-Akt1 and FAK-PS, respectively. Histogram of binding forces of FAK-Akt1 at different contact levels: 1 nm (a), 3 nm (b), 5 nm (c), 10 nm (d). Histogram of binding forces of FAK-PS at different contact levels: 1 nm (e), 3 nm (f), 5 nm (g), 10 nm (h).

1) AFM tip-substrate contact level

AFM tip-substrate contact level affects the distribution of the binding forces between FAK-Akt1 molecular pairs. AFM tip contact level is related to the size of interface between surface molecules on the AFM probe and the substrate. Enlarging this interface will increase the number of FAK-Akt1 molecular pairs, which tends to increase the measured binding forces. To test this hypothesis, four contact levels were tested: 1 nm, 3 nm, 5 nm, and 10 nm. In FAK-PS negative control groups, tip contact depth affected the binding force minimally. As the depth increased from 1 nm to 10 nm, larger binding forces emerged; however, the majority of the measured binding force is concentrated at 30 pN, which can be interpreted as noise (FAK-PS in Fig. 3 (e-h)). On the other hand, measured binding forces between FAK-Akt1 molecular pairs increased significantly with the increased contact levels. The peaks of the distribution were located at around 50 pN and 130 pN for 1 nm contact level, around 70 pN and 150 pN for 3 nm contact level, around 80 pN and 110 pN for 5 nm contact level, and around 80 pN, 144 pN and 215 pN for 10 nm contact level (Fig. 3 (a-d)).

2) AFM tip-substrate contact time

Forming specific binding requires a particular orientation of the molecular pairs. Considering the time cost of orienting molecules, forming a specific binding might require a much longer time than forming a non-specific binding [56]. We therefore evaluated the effect of tip-substrate contact time on the measured binding force. Two tip-substrate contact times were tested: 500 ms and 1000 ms. In FAK-PS negative control group, the binding force histogram distribution maintained the same pattern with the two contact times: 98% and 93% of measured binding force is concentrated around peaks at 24 pN and 36 pN for contact times of 500 ms and 1000 ms, respectively (FAK-PS, Fig. 4). In FAK-Akt1 experimental groups, the binding forces of FAK-Akt1 interactions are increased significantly. Two peaks occurred at 50 pN and 70 pN when the contact time increasing from 500 ms to 1000 ms (Fig. 4 (b)).

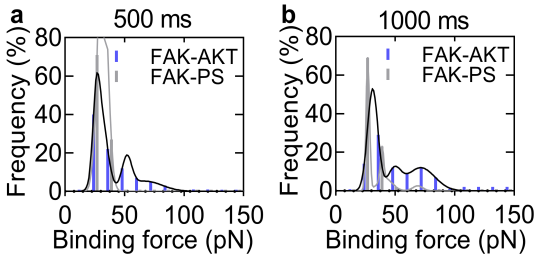

Fig. 4. Optimization of the tip-substrate contact time. (a-b) Histogram of binding forces between FAK-Akt1 (blue bars) and FAK-PS (gray bars) with tip-substrate contact time as 500 ms (a) and 1000 ms (b).

3) AFM tip moving speed

It has been reported that the moving speed of AFM tip affected the measured binding force significantly [57-59]. Increasing the tip moving speed increases the SNR [38]. Three moving speeds of the AFM tip were tested: 100 nm/s, 200 nm/s, and 400 nm/s. In the FAK-PS case, the non-specific binding force increased as the moving speed of AFM tip is increased (FAK-PS, Fig. 5 (a-c)). However, this influence is minimal, as the binding forces mainly distributed in the range from 20 pN to 40 pN; 97%, 94%, and 87% for tip moving speeds of 100 nm/s, 200 nm/s, and 400 nm/s, respectively, which is consistent with previous reports [58, 60]. In the FAK-Akt1 case, however, the best measurement occurred at a medium speed level, 200 nm/s (FAK-AKT, Fig. 5 (a-c)). At the speed of 200 nm/s, the measured FAK-Akt1 interactions exhibited a Gaussian distribution (Fig. 5 (b)). The peaks of the binding force are located at 60 pN and 80 pN for tip moving at 100 nm/s and 200 nm/s. Two distribution peaks existed at 50 pN and 90 pN for tip moving speed at 400 nm/s. At the speed of 400 nm/s, the binding force at 30 pN, which interpreted as non-specific binding, increased to more than 50% compared (Fig. 5 (c)) with 30% and less than 5% at the tip moving speed at 100 nm/s and 200 nm/s (Fig. 5 (a and b)).

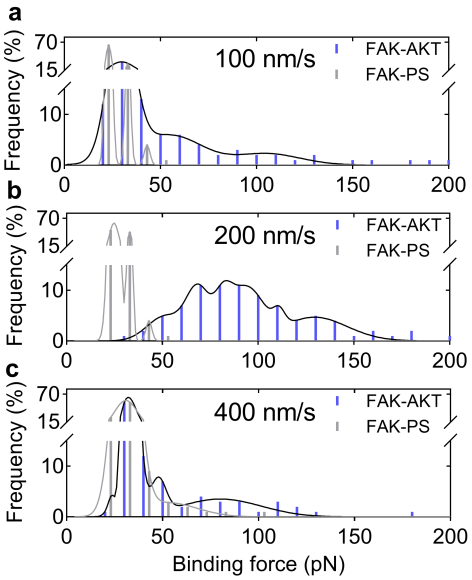

Fig. 5. Optimization of tip moving speed. Histogram of FAK-Akt1 and FAK-PS binding forces with tip moving speeds at 100 nm/s (a), 200 nm/s (b), and 400 nm/s (c).

C. Statistical analysis-based data processing

Besides optimizing the experimental conditions, data processing and visualization methods also affects the perceived SNR. Assuming that the molecules on AFM tip has the same probabilities to form molecular pairs with the molecules on the substrate, the measured AFM force spectroscopy data follow a Poisson distribution [61-63]. After mathematical manipulation, the binding force of single molecular pair can be estimated by the following equation [61]:

$$\mu_m = \mu_n F_i + F_0 \quad (1)$$

$$\sigma_m^2 = \sigma_n^2 * F_i^2 = \mu_m F_i - F_i F_0 \quad (2)$$

In this equation, μ_m and σ_m^2 are the mean and standard deviation of the measured binding forces, F_i is the binding force of a single molecular pair, μ_n is the mean number of molecular pairs formed, and F_0 is the sum of all non-specific bindings. A linear regression analysis of the measured data reveals the

binding force of a single molecular pair, F_i . Assuming F_i does not change during the experiment, the experimental data with larger measured binding force will also have a larger standard deviation. Considering the binding force in experimental groups (FAK-Akt1) is much larger than that in negative control groups, the standard deviation should increase much faster in FAK-Akt1 than that in FAK-PS groups. Here we presented the mean value and standard deviation of the experimental data in different experimental conditions: the level and time of tip-substrate contact and AFM tip moving speeds. In all experimental conditions, the mean value of experimental and control groups is approximately 63.1 ± 24.7 pN, and 27.5 ± 2.8 pN (mean ± SD), respectively (Fig. 6 (a, c, and e)). However, the standard deviation varies 10 to 100 times between these two groups (Fig. 6 (b, d, and f)). On average, the standard deviations of FAK-Akt1 and FAK-PS binding forces are 2311.1 ± 1226.1 pN^2 and 70.7 ± 75.5 pN^2, respectively. Thus, the standard deviation is a better parameter to enhance the contrast between experimental and negative control groups in screening drug candidates, as shown in Fig. 6.

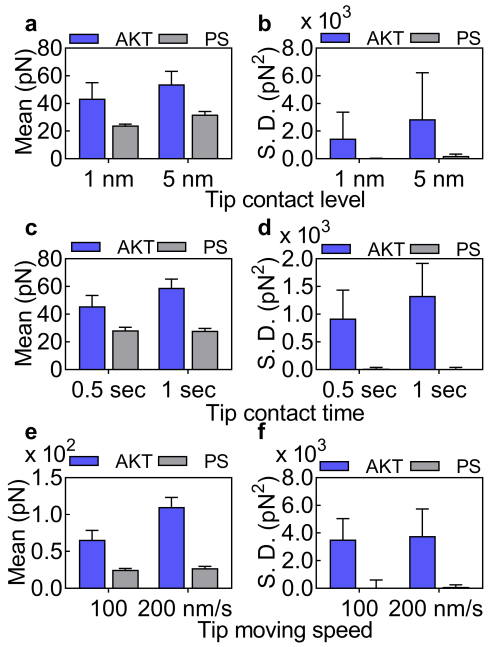

Fig. 6. Standard deviation (SD) of binding force data presents the FAK-Akt1 and FAK-PS binding force with high contrast. (a, c and e) the mean of FAK-Akt1 and FAK-PS binding forces with different: (a) tip-substrate contact levels, (c) tip-substrate contact times, and (e) tip moving speeds. (b, d and f) the mean of FAK-Akt1 and FAK-PS binding forces with different: (b) tip-substrate contact levels, (d) tip indentation times, and (f) tip moving speeds.

IV. DISCUSSION

In this research, the substrate functionalization method and tip-substrate contact regime have been optimized to improve the SNR when measuring protein-protein interactions. Three factors in tip-substrate contact regime were optimized: the level and time of tip-substrate contact, and the tip moving speed before and after tip-substrate contact.

Directly depositing protein molecules onto PS substrates via hydrophobic interactions generates a uniform protein layer. One concern that might be raised is whether a monolayer of Akt1 molecules were deposited or not. We did not specifically prove that this deposition process creates a monolayer of molecules. However, we are ultimately trying to model FAK-Akt1 interaction in living cells, where there are neither monolayers nor multilayers of Akt1, but where multiple different molecules may interact in suspension within the cytosol or in multi-protein complexes.

The measured protein-protein interactions with the new substrate functionalization method is in the same range reported previously. Specifically, there have been reports showing that non-specific binding forces below 10 pN [22]. Although, we have not been able to find publications reporting the binding force between FAK and Akt1 molecules, with repeated experiments showing the peak binding forces at 80 pN, we have no reason to believe it is not the interaction force between FAK and Akt1. In fact, this force falls in the same range as other binding forces between a pair of protein molecules with affinity [22, 27].

Discrete Fourier transform, implemented by Fast Fourier transform (FFT), illuminates the periodic characters in discrete input data sequence as well as the relative strengths of each periodic component. The experimental data were analyzed by FFT to reveal their frequency distributions. Increasing tip-substrate contact levels narrowed the frequency distribution in negative control groups, FAK-PS. (Fig. 7 (a)). Larger binding forces emerged in deeper contact levels and expanded the range of measured binding forces. This enlarged range of force distributions decreases the energy at high frequencies. In the FAK-Akt1 group, increasing tip contact depth changed the distribution dramatically. As the contact depth increased, the relative amplitude strengths of higher frequencies increased. This means that more peaks with a small period exist. This is consistent with the analysis of the distribution. These results indicate that increasing contact depth increased the observed binding forces by forming more interacting molecular pairs. Together with the histogram data, FFT analysis results revealed that contact depth affects binding forces in the FAK-Akt1 experimental groups than that in the FAK-PS negative control groups. Furthermore, compared with other contact levels, the contact level of 5 nm has unique characteristics. In both FAK-Akt1 and FAK-PS groups, the amplitude at high frequencies keep at low level. This character also presented as a single peak in the histogram (Fig. 3 (c and g)). Based on these results, we selected a depth of 5 nm for further experiment.

Regarding the tip-substrate contact time, FFT analysis further confirmed the minimal effect of contact time for negative control groups, with two curves almost overlapping with each other. (Fig. 7 (c)). This result is consistent with previous report [56]. In the FAK-Akt1 groups, however, increasing tip-substrate contact time elevated the measured binding force significantly. The frequencies at larger binding forces increased at longer contact time. Binding and unbinding of FAK-Akt1 molecular pairs are dynamic processes, which require specific orientation of the target molecules. A longer reaction time permits the formation of more binding events before the reaction reaches equilibrium. FFT analysis presented

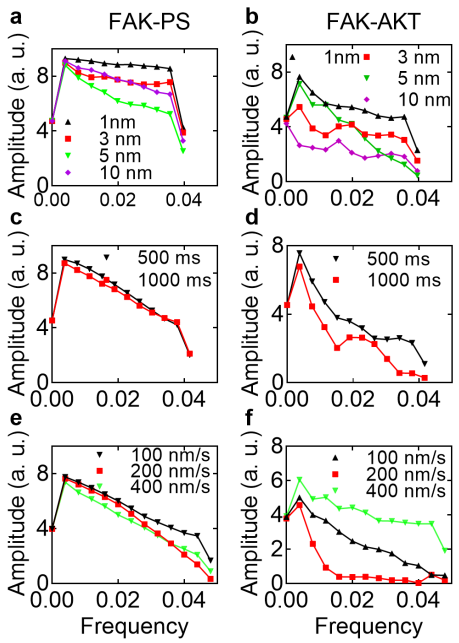

Fig. 7. Fast Fourier transform (FFT) analysis of the histogram data from measured binding forces in various experimental conditions. (a, b) FFT of the histogram data of binding forces between FAK-Akt1 (a) and FAK-PS (b) at different tip-substrate contact levels. (c, d) FFT of the histogram data of binding forces between FAK-Akt1 (c) and FAK-PS (d) with different tip-substrate contact times. (e, f) FFT of the histogram data of binding forces between FAK-Akt1 (e) and FAK-PS (f) with the three tip moving speeds.

a peak at 0.027 pN^{-1} (Fig. 7 (d)), which represent that a high component of period of 37 pN. This is consistent with histogram analysis.

Regarding the tip moving speeds during tip-substrate contact, in the FAK-PS group, as the moving speed increased, the percentage of binding forces at 20 pN is transferred to 30 pN and 40 pN. The FFT analysis also confirmed that the tip moving speed affected the binding force minimally in the negative control groups (Fig. 7 (e)). In the FAK-Akt1 group, FFT results revealed that most of the energy is distributed in low frequency ranges with tip moving speed at 200 nm/s, which is consistent with the single Gaussian distribution (Fig. 7 (e)). At 200 nm/s, the SNR improved dramatically, as the overlap area between FAK-PS and FAK-AKT1 groups was significantly reduced. The average of FAK-AKT1 binding force is around 3 times larger than that of the FAK-PS group (Fig. 6(e)). Considering the standard deviation of the binding forces as the signal (Fig. 6(f)), the signal is 80 times larger than that of the noise, as the standard deviation of the FAK-PS group. These results demonstrated that the methods improved the SNR significantly compared with previous reports [37, 38].

The existence of an optimal tip moving speed differs from the theoretical analysis in the literature which suggests that faster tip moving speed induces stronger binding forces [58, 59]. This change might be due to the differences in experimental conditions. In previous studies, molecules were fixed to the substrate via a linker molecule or on gold surface [29, 64]. The Akt1 molecules in the current study were directly deposited onto the substrate via hydrophobic interactions. The structure of a complex organic molecule will change during forming and breaking a molecular bond, which affects the number of available hydrophobic sites. The high rates of non-specific bindings in experimental group with 400 nm/s tip moving speed, indicated that the Akt1 molecules might be released from PS substrate. Collectively, these results demonstrated that an optimum moving speed exists for measuring the binding force in current experimental condition. Further mechanistic analysis is needed to fully understand this process.

This statistical analysis method for presenting the data also reveals new insights for the influences of different parameters on the measured binding forces. Increasing the tip-substrate contact level increases the mean value, 23.3% and 33% in FAK-Akt1 and FAK-PS groups, respectively (Fig. 6 (a, b)). However, the standard deviation increases 94% and 85.4%, respectively. This means that contact depths increase the noises more than the signals. Tip-substrate contact time minimally affects negative control groups but increases the mean and standard deviation in the experimental group 29.1% and 14.7%, respectively (Fig. 6 (c, d)). This means that tip-substrate contact time mainly amplifies the signal with little effect on the noise level. The tip moving speed increases the mean value of the measured binding forces but does not affect their standard deviation in FAK-Akt1 groups. This is consistent with the data in the histogram. Moving speed mainly shifts the peak right and does not affect the range (Fig. 6 (e, f)). According to (2), this can be interpreted as the tip moving speed elevating the measured binding forces of a single molecular pair, consistent with previous models [59].

Certainly, there is more work to be done to combine all these advances to utilize AFM force spectroscopy as a high throughput screening technology. However, throughput may be a big hurdle if large numbers of replicates are required. We therefore sought here to improve the efficiency and effectiveness of the screening process itself by enhancing the SNR. In this way, the total number of force curves required to generate an identifiable contrast between experimental and control groups will be significantly reduced, thus increasing the throughput of this screening method.

V. Conclusion and Future Perspectives

In sum, toward developing an effective and efficient high throughput screening method for drug discovery using AFM force spectroscopy, the experimental settings were optimized to improve the SNR in screening protein-protein interactions. New substrate functionalization method was developed to reduce the noises. Experimental parameters, including the level and time of tip-substrate contact and tip moving speeds, were optimized towards this application to enhance the SNR. A new data processing method based on statistical analysis was also developed to enhance the contrast between experimental and control groups. Collectively, these techniques may facilitate the development of an AFM based high throughput screening system.

Further, besides the high sensitivity of AFM force spectroscopy, it can also integrate with other biosensing or sample handling technologies. Integrating with microfluidics,

the molecules involved in the screening process can be in small volume and be changed in a fast manner [65]. To minimize the size of the device and to simplify the design, the complicated laser based position sensing device can be replace by piezoelectric sensing device [66]. Fluorescence based biosensor can also be integrated with AFM force spectroscopy to characterize the protein-protein interaction both at single molecular and large volume level. These progresses, parallelizing and automating the system operation, integrating with other biosensing and system-enabling technologies, and optimizing interaction regimes presented in this paper, altogether formed a concrete foundation to develop an AFM force spectroscopy-enabled high-throughput screening of protein-protein interactions for drug discovery.

ACKNOWLEDGMENT

We, the authors, thank Dr. Mi Li for his help in experimental techniques. We thank Dr. Jing Yu for her help on arranging the experiments.

REFERENCES

[1] H.-P. Shih, X. Zhang, and A. M. Aronov, "Drug discovery effectiveness from the standpoint of therapeutic mechanisms and indications," *Nature Reviews Drug Discovery,* vol. 17, pp. 19, 10/27/online, 2017.

[2] S. M. Paul, D. S. Mytelka, C. T. Dunwiddie, C. C. Persinger, B. H. Munos, S. R. Lindborg, and A. L. Schacht, "How to improve R&D productivity: the pharmaceutical industry's grand challenge," *Nature Reviews Drug Discovery,* vol. 9, pp. 203, 2010.

[3] F. Pammolli, L. Magazzini, and M. Riccaboni, "The productivity crisis in pharmaceutical R&D," *Nature Reviews Drug Discovery,* vol. 10, pp. 428, 06/01/online, 2011.

[4] J. D. Hood, and D. A. Cheresh, "Role of integrins in cell invasion and migration," *Nature Reviews Cancer,* vol. 2, no. 2, pp. 91-+, Feb, 2002.

[5] L. Blanchoin, R. Boujemaa-Paterski, C. Sykes, and J. Plastino, "ACTIN DYNAMICS, ARCHITECTURE, AND MECHANICS IN CELL MOTILITY," *Physiological Reviews,* vol. 94, no. 1, pp. 235-263, Jan, 2014.

[6] K. H. Bleicher, H.-J. Böhm, K. Müller, and A. I. Alanine, "Hit and lead generation: beyond high-throughput screening," *Nature Reviews Drug Discovery,* vol. 2, pp. 369, 05/01/online, 2003.

[7] J. P. Renaud, C. W. Chung, U. H. Danielson, U. Egner, M. Hennig, R. E. Hubbard, and H. Nar, "Biophysics in drug discovery: impact, challenges and opportunities," *Nature Reviews Drug Discovery,* vol. 15, no. 10, pp. 679-698, Oct, 2016.

[8] M. Zhou, Q. Li, and R. Wang, "Current Experimental Methods for Characterizing Protein–Protein Interactions," *ChemMedChem,* vol. 11, no. 8, pp. 738-756, 2016.

[9] Y. Bai, Q. Luo, and J. Liu, "Protein self-assembly via supramolecular strategies," *Chemical Society Reviews,* vol. 45, no. 10, pp. 2756-2767, 2016.

[10] M. R. Arkin, and J. A. Wells, "Small-molecule inhibitors of protein–protein interactions: progressing towards the dream," *Nature Reviews Drug Discovery,* vol. 3, pp. 301, 04/01/online, 2004.

[11] M. B. Rone, J. Fan, and V. Papadopoulos, "Cholesterol transport in steroid biosynthesis: Role of protein–protein interactions and implications in disease states," *Biochimica et Biophysica Acta (BBA) - Molecular and Cell Biology of Lipids,* vol. 1791, no. 7, pp. 646-658, 2009/07/01/, 2009.

[12] D. E. Scott, A. R. Bayly, C. Abell, and J. Skidmore, "Small molecules, big targets: drug discovery faces the protein–protein interaction challenge," *Nature Reviews Drug Discovery,* vol. 15, pp. 533, 04/11/online, 2016.

[13] P. Thiel, M. Kaiser, and C. Ottmann, "Small-Molecule Stabilization of Protein–Protein Interactions: An Underestimated Concept in Drug Discovery?," *Angewandte Chemie International Edition,* vol. 51, no. 9, pp. 2012-2018, 2012/02/27, 2012.

[14] A. Mullard, "Protein–protein interaction inhibitors get into the groove," *Nature Reviews Drug Discovery,* vol. 11, pp. 173, 03/01/online, 2012.

[15] M. A. Cooper, "Optical biosensors in drug discovery," *Nature Reviews Drug Discovery,* vol. 1, pp. 515, 07/01/online, 2002.

[16] R. F. Curpan, P. C. Simons, D. Zhai, S. M. Young, M. B. Carter, C. G. Bologa, T. I. Oprea, A. C. Satterthwait, J. C. Reed, B. S. Edwards, and L. A. Sklar, "High-Throughput Screen for the Chemical Inhibitors of Antiapoptotic Bcl-2 Family Proteins by Multiplex Flow Cytometry," *ASSAY and Drug Development Technologies,* vol. 9, no. 5, pp. 465-474, 2011/10/01, 2011.

[17] M. R. Arkin, Y. Tang, and J. A. Wells, "Small-molecule inhibitors of protein-protein interactions: progressing toward the reality," *Chem Biol,* vol. 21, no. 9, pp. 1102-14, Sep 18, 2014.

[18] N. Wakabayashi, S. Shin, S. L. Slocum, E. S. Agoston, J. Wakabayashi, M.-K. Kwak, V. Misra, S. Biswal, M. Yamamoto, and T. W. Kensler, "Regulation of Notch1 Signaling by Nrf2: Implications for Tissue Regeneration," *Science Signaling,* vol. 3, no. 130, pp. ra52-ra52, 2010.

[19] S. Cialfi, R. Palermo, S. Manca, C. De Blasio, P. V. Romero, S. Checquolo, D. Bellavia, D. Uccelletti, M. Saliola, A. D'Alessandro, L. Zolla, A. Gulino, I. Screpanti, and C. Talora, "Loss of Notch1-dependent p21(Waf1/Cip1) expression influences the Notch1 outcome in tumorigenesis," *Cell Cycle,* vol. 13, no. 13, pp. 2046-2055, Jul 1, 2014.

[20] P.-J. Hsiao, J.-C. Jao, J.-L. Tsai, W.-T. Chang, K.-S. Jeng, and K.-K. Kuo, "Inorganic arsenic trioxide induces gap junction loss in association with the downregulation of connexin43 and E-cadherin in rat hepatic "stem-like" cells," *The Kaohsiung Journal of Medical Sciences,* vol. 30, no. 2, pp. 57-67, 2014/02/01/, 2014.

[21] J. Nriagu, T.-S. Lin, D. G. Mazumder, and D. Chatterjee, "E-cadherin polymorphisms and susceptibility to arsenic-related skin lesions in West Bengal, India," *Science of The Total Environment,* vol. 420, pp. 65-72, 2012.

[22] Kevin C. Patterson, R. Yang, B. Zeng, B. Song, S. Wang, N. Xi, and Marc D. Basson, "Measurement of Cationic and Intracellular Modulation of Integrin Binding Affinity by AFM-Based Nanorobot," *Biophysical Journal,* vol. 105, no. 1, pp. 40-47, 2013/07/02/, 2013.

[23] Y. Yang, J. Yu, A. M. Esfahani, K. Seiffert-Sinha, N. Xi, I. Lee, A. A. Sinha, L. Chen, Z. Sun, and R. Yang, "Single-Cell Membrane Drug Delivery using Porous Pen Nanodeposition," *Nanoscale*, 2018.

[24] F. A. Scaramuzzo, R. Salvati, B. Paci, A. Generosi, V. Rossi-Albertini, A. Latini, and M. Barteri, "Nanoscale In Situ Morphological Study of Proteins Immobilized on Gold Thin Films," *The Journal of Physical Chemistry B,* vol. 113, no. 48, pp. 15895-15899, 2009/12/03, 2009.

[25] C. Stroh, H. Wang, R. Bash, B. Ashcroft, J. Nelson, H. Gruber, D. Lohr, S. M. Lindsay, and P. Hinterdorfer, "Single-molecule recognition imaging microscopy," *Proceedings of the National Academy of Sciences of the United States of America,* vol. 101, no. 34, pp. 12503-12507, 2004.

[26] L. Lin, H. Wang, Y. Liu, H. Yan, and S. Lindsay, "Recognition Imaging with a DNA Aptamer," *Biophysical Journal,* vol. 90, no. 11, pp. 4236-4238, 2006/06/01/, 2006.

[27] S. Senapati, S. Manna, S. Lindsay, and P. Zhang, "Application of Catalyst-Free Click Reactions in Attaching Affinity Molecules to Tips of Atomic Force Microscopy for Detection of Protein Biomarkers," *Langmuir,* vol. 29, no. 47, pp. 14622-14630, 2013/11/26, 2013.

[28] A. Fahs, and G. Louarn, "Plant protein interactions studied using AFM force spectroscopy: nanomechanical and adhesion properties," *Physical Chemistry Chemical Physics,* vol. 15, no. 27, pp. 11339-11348, 2013.

[29] C. McAllister, M. A. Karymov, Y. Kawano, A. Y. Lushnikov, A. Mikheikin, V. N. Uversky, and Y. L. Lyubchenko, "Protein Interactions and Misfolding Analyzed by AFM Force Spectroscopy," *Journal of Molecular Biology,* vol. 354, no. 5, pp. 1028-1042, 2005/12/16/, 2005.

[30] W. Hu, C. M. Li, X. Cui, H. Dong, and Q. Zhou, "In Situ Studies of Protein Adsorptions on Poly(pyrrole-co-pyrrole propylic acid) Film

by Electrochemical Surface Plasmon Resonance," *Langmuir,* vol. 23, no. 5, pp. 2761-2767, 2007/02/01, 2007.

[31] F. Oesterhelt, M. Rief, and H. E. Gaub, "Single molecule force spectroscopy by AFM indicates helical structure of poly(ethylene-glycol) in water," *New Journal of Physics,* vol. 1, no. 1, pp. 6, 1999.

[32] M. C. Leake, "The physics of life: one molecule at a time," *Philosophical Transactions of the Royal Society B-Biological Sciences,* vol. 368, no. 1611, Feb 5, 2013.

[33] K.-B. Lee, S.-J. Park, C. A. Mirkin, J. C. Smith, and M. Mrksich, "Protein Nanoarrays Generated By Dip-Pen Nanolithography," *Science,* vol. 295, no. 5560, pp. 1702, 2002.

[34] Patrick D. Bosshart, Patrick L. T. M. Frederix, and A. Engel, "Reference-Free Alignment and Sorting of Single-Molecule Force Spectroscopy Data," *Biophysical Journal,* vol. 102, no. 9, pp. 2202-2211, 2012/05/02/, 2012.

[35] C. Ignacio, and S. Simon, "Automated setpoint adjustment for biological contact mode atomic force microscopy imaging," *Nanotechnology,* vol. 21, no. 3, pp. 035104, 2010.

[36] S. Jens, W. Reiner, L. Mirko, N. Joao, J. Harald, G. Ulrich, H. Gerd, J. Torsten, and J. M. Daniel, "Fully automated single-molecule force spectroscopy for screening applications," *Nanotechnology,* vol. 19, no. 38, pp. 384020, 2008.

[37] W. Baumgartner, P. Hinterdorfer, and H. Schindler, "Data analysis of interaction forces measured with the atomic force microscope," *Ultramicroscopy,* vol. 82, no. 1, pp. 85-95, 2000/02/01/, 2000.

[38] C. P. Calderon, W.-H. Chen, K.-J. Lin, N. C. Harris, and C.-H. Kiang, "Quantifying DNA melting transitions using single-molecule force spectroscopy," *Journal of Physics: Condensed Matter,* vol. 21, no. 3, pp. 034114, 2008/12/17, 2008.

[39] T. Machleidt, C. C. Woodroofe, M. K. Schwinn, J. Méndez, M. B. Robers, K. Zimmerman, P. Otto, D. L. Daniels, T. A. Kirkland, and K. V. Wood, "NanoBRET—A Novel BRET Platform for the Analysis of Protein–Protein Interactions," *ACS Chemical Biology,* vol. 10, no. 8, pp. 1797-1804, 2015/08/21, 2015.

[40] B. C. Collins, C. L. Hunter, Y. Liu, B. Schilling, G. Rosenberger, S. L. Bader, D. W. Chan, B. W. Gibson, A.-C. Gingras, J. M. Held, M. Hirayama-Kurogi, G. Hou, C. Krisp, B. Larsen, L. Lin, S. Liu, M. P. Molloy, R. L. Moritz, S. Ohtsuki, R. Schlapbach, N. Selevsek, S. N. Thomas, S.-C. Tzeng, H. Zhang, and R. Aebersold, "Multi-laboratory assessment of reproducibility, qualitative and quantitative performance of SWATH-mass spectrometry," *Nature Communications,* vol. 8, no. 1, pp. 291, 2017/08/21, 2017.

[41] A. Abumazwed, W. Kubo, C. Shen, T. Tanaka, and A. G. Kirk, "Projection method for improving signal to noise ratio of localized surface plasmon resonance biosensors," *Biomedical Optics Express,* vol. 8, no. 1, pp. 446-459, 2017/01/01, 2017.

[42] M. A. Beuwer, M. W. J. Prins, and P. Zijlstra, "Stochastic Protein Interactions Monitored by Hundreds of Single-Molecule Plasmonic Biosensors," *Nano Letters,* vol. 15, no. 5, pp. 3507-3511, 2015/05/13, 2015.

[43] A. L. Garner, "cat-ELCCA: catalyzing drug discovery through click chemistry," *Chemical Communications,* vol. 54, no. 50, pp. 6531-6539, 2018.

[44] C. P. Gayer, and M. D. Basson, "The effects of mechanical forces on intestinal physiology and pathology," *Cellular Signalling,* vol. 21, no. 8, pp. 1237-1244, Aug, 2009.

[45] S. Y. Wang, and M. D. Basson, "Akt directly regulates focal adhesion kinase through association and serine phosphorylation: implication for pressure-induced colon cancer metastasis," *American Journal of Physiology-Cell Physiology,* vol. 300, no. 3, pp. C657-C670, Mar, 2011.

[46] W. C. Conway, J. Van der Voort van Zyp, V. Thamilselvan, M. F. Walsh, D. L. Crowe, and M. D. Basson, "Paxillin modulates squamous cancer cell adhesion and is important in pressure-augmented adhesion," *Journal of Cellular Biochemistry,* vol. 98, no. 6, pp. 1507-1516, 2006.

[47] S. K. Mitra, D. A. Hanson, and D. D. Schlaepfer, "Focal adhesion kinase: In command and control of cell motility," *Nature Reviews Molecular Cell Biology,* vol. 6, no. 1, pp. 56-68, Jan, 2005.

[48] D. R. Germolec, T. Yoshida, K. Gaido, J. L. Wilmer, P. P. Simeonova, F. Kayama, F. Burleson, W. Dong, R. W. Lange, and M. I. Luster, "Arsenic induces overexpression of growth factors in human keratinocytes," *Toxicology and Applied Pharmacology,* vol. 141, no. 1, pp. 308-318, 1996/11/01/, 1996.

[49] J. L. Hutter, and J. Bechhoefer, "Calibration of atomic‐force microscope tips," *Review of Scientific Instruments,* vol. 64, no. 7, pp. 1868-1873, 1993.

[50] B. Kasemo, "Biological surface science," *Surface science,* vol. 500, no. 1, pp. 656-677, 2002.

[51] Y. Yang, J. Volmering, M. Junkin, and P. K. Wong, "Comparative assembly of colloidal quantum dots on surface templates patterned by plasma lithography," *Soft matter,* vol. 7, no. 21, pp. 10085-10090, 2011.

[52] R. Kumar, S. N. Ramakrishna, V. V. Naik, Z. Chu, M. E. Drew, N. D. Spencer, and Y. Yamakoshi, "Versatile method for AFM-tip functionalization with biomolecules: fishing a ligand by means of an in situ click reaction," *Nanoscale,* vol. 7, no. 15, pp. 6599-6606, 2015/04/21/, 2015.

[53] K. Awsiuk, A. Budkowski, A. Psarouli, P. Petrou, A. Bernasik, S. Kakabakos, J. Rysz, and I. Raptis, "Protein adsorption and covalent bonding to silicon nitride surfaces modified with organo-silanes: Comparison using AFM, angle-resolved XPS and multivariate ToF-SIMS analysis," *Colloids and Surfaces B: Biointerfaces,* vol. 110, pp. 217-224, 2013/10/01/, 2013.

[54] N. Crampton, W. A. Bonass, J. Kirkham, and N. H. Thomson, "Formation of Aminosilane-Functionalized Mica for Atomic Force Microscopy Imaging of DNA," *Langmuir,* vol. 21, no. 17, pp. 7884-7891, 2005/08/01, 2005.

[55] N. Gartmann, C. Schutze, H. Ritter, and D. Bruhwiler, "The Effect of Water on the Functionalization of Mesoporous Silica with 3-Aminopropyltriethoxysilane," *Journal of Physical Chemistry Letters,* vol. 1, no. 1, pp. 379-382, Jan, 2010.

[56] E. Celik, and V. T. Moy, "Nonspecific interactions in AFM force spectroscopy measurements," *Journal of Molecular Recognition,* vol. 25, no. 1, pp. 53-56, 2012.

[57] M. Schlierf, and M. Rief, "Single-molecule unfolding force distributions reveal a funnel-shaped energy landscape," *Biophysical Journal,* vol. 90, no. 4, pp. L33-L35, Feb, 2006.

[58] O. K. Dudko, G. Hummer, and A. Szabo, "Theory, analysis, and interpretation of single-molecule force spectroscopy experiments," *Proceedings of the National Academy Of Sciences,* vol. 105, no. 41, pp. 15755-15760, October 14, 2008, 2008.

[59] J. T. Bullerjahn, S. Sturm, and K. Kroy, "Theory of rapid force spectroscopy," *Nature communications,* vol. 5, 2014.

[60] Y.-S. Lo, Y.-J. Zhu, and T. P. Beebe, "Loading-Rate Dependence of Individual Ligand−Receptor Bond-Rupture Forces Studied by Atomic Force Microscopy," *Langmuir,* vol. 17, no. 12, pp. 3741-3748, 2001/06/01, 2001.

[61] J. M. Williams, T. Han, and T. P. Beebe, "Determination of Single-Bond Forces from Contact Force Variances in Atomic Force Microscopy," *Langmuir,* vol. 12, no. 5, pp. 1291-1295, 1996/01/01, 1996.

[62] F. Stevens, Y.-S. Lo, J. M. Harris, and T. P. Beebe, "Computer Modeling of Atomic Force Microscopy Force Measurements: Comparisons of Poisson, Histogram, and Continuum Methods," *Langmuir,* vol. 15, no. 1, pp. 207-213, 1999/01/01, 1999.

[63] L. A. Wenzler, G. L. Moyes, L. G. Olson, J. M. Harris, and T. P. Beebe, "Single-Molecule Bond-Rupture Force Analysis of Interactions between AFM Tips and Substrates Modified with Organosilanes," *Analytical Chemistry,* vol. 69, no. 14, pp. 2855-2861, 1997/07/01, 1997.

[64] G. Neuert, C. Albrecht, E. Pamir, and H. E. Gaub, "Dynamic force spectroscopy of the digoxigenin–antibody complex," *FEBS Letters,* vol. 580, no. 2, pp. 505-509, 2006.

[65] S. Kim, K. D. Kihm, and T. Thundat, "Fluidic applications for atomic force microscopy (AFM) with microcantilever sensors," *Experiments in Fluids,* vol. 48, no. 5, pp. 721-736, 2010/05/01, 2010.

[66] L. Gonzalez, M. Rodrigues, A. M. Benito, L. Pérez-García, M. Puig-Vidal, and J. Otero, "Piezoelectric tuning fork biosensors for the quantitative measurement of biomolecular interactions," *Nanotechnology,* vol. 26, no. 49, pp. 495502, 2015.